

Distributed Bragg reflector consisting of high- and low-refractive-index thin film layers made of the same material

Martin F. Schubert, J.-Q. Xi, Jong Kyu Kim, and E. Fred Schubert^{a)}

Department of Electrical, Computer, and Systems Engineering, Rensselaer Polytechnic Institute, Troy, New York 12180

(Received 2 February 2007; accepted 5 March 2007; published online 6 April 2007)

A conductive distributed Bragg reflector (DBR) composed entirely of a single material—indium tin oxide (ITO)—is reported. The high- and low-refractive-index layers of the DBR are deposited by oblique-angle deposition and consist of ITO thin films with low and high porosities, which yield an index contrast of $\Delta n=0.4$. A single-material DBR with three periods achieves a reflectivity of 72.7%, in excellent agreement with theory. © 2007 American Institute of Physics.

[DOI: 10.1063/1.2720269]

Oblique-angle deposition allows the fabrication of nanostructured porous low-refractive-index (low- n) thin films of high optical quality. Films fabricated by oblique-angle deposition have refractive index values which can bridge the gap between conventional solid materials ($n \geq 1.4$) and air ($n=1.0$). Using this technique with SiO_2 , we have achieved refractive index values as low as 1.08.¹ A material with refractive index so close to that of free space can enhance performance in many photonics applications, such as broadband antireflection coatings with air ambient,^{2–4} omnidirectional reflectors,^{5,6} distributed Bragg reflectors (DBRs),^{7,8} optical microresonators,^{9,10} light-emitting diodes (LEDs),¹¹ and optical interconnects.¹² Oblique-angle deposition has also been applied to realize optical thin film components which consist of a single material.^{13–15} In these cases fabrication by oblique-angle deposition of a single material is used to achieve fine-grained control over the refractive index or to simplify fabrication.

In this letter we show that oblique-angle deposition can also be used to fabricate optical components with properties that are difficult to realize by conventional two-material approaches. Thin film optical structures generally consist of several layers of different materials with different refractive indices. However, the refractive index and other properties of a material such as conductivity and optical absorption are in general inextricably coupled. Due to the limited number of available materials, the choice of refractive index also dictates remaining material characteristics. For photonics applications that exploit both optical and electrical properties of a material, this can force unsatisfactory compromises. By controlling the deposition angle and thereby the layer porosity and refractive index, oblique-angle deposition allows the fabrication of thin film components composed of a single material chosen for its electrical or other properties in which each layer has different refractive index that is individually tuned to a specific desired value. This ability is crucial when material properties in addition to the refractive index are important. As proof of concept, we demonstrate a conductive DBR designed for 460 nm operation made from indium tin oxide (ITO) fabricated using the oblique-angle deposition technique.

A DBR is a highly reflective mirror which consists of alternating layers of high- and low-index films, each having a quarter-wavelength thickness. DBRs are used in a variety of photonics applications such as high efficiency LEDs^{16–18} and vertical-cavity surface-emitting lasers.^{19,20} The reflectivity of a DBR is highest when the difference in refractive index between the high- and low-refractive-index layers is maximized. Therefore, the very low refractive indices—and by extension, high-index contrast—achievable by varying the deposition angle make DBRs excellent candidates for the application of oblique-angle deposition. In conventional DBR structures the high-index and low-index layers are composed of two different materials such as TiO_2 and SiO_2 . However, neither TiO_2 nor SiO_2 is electrically conductive. Commonly used conductive DBRs are limited to epitaxially grown doped semiconductors, which generally have low-index contrast. In addition, some materials may not work at certain wavelengths due to absorption. The DBR reported here is composed of ITO—which is both conductive and transparent at 460 nm—and serves as an example of the design freedom afforded by oblique-angle deposition for optical thin film components.

ITO films are deposited on silicon substrate at angles ranging from 0° to 75° using electron-beam evaporation and characterized by ellipsometry, scanning-electron microscopy (SEM), and optical microscopy. After deposition, the samples are annealed for 1 min at 500°C in an oxygen atmosphere. Figure 1 shows a schematic of the deposition setup. At large vapor incident angles, deposited particles cast a shadow over a portion of the substrate and prevent additional deposition in these areas. Incoming particles are not deposited in the shadowed regions, which results in the formation of a porous nanorod film. If the voids in the porous

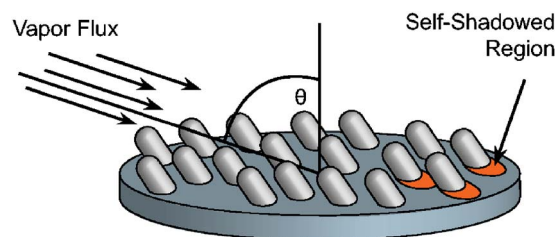


FIG. 1. (Color online) Schematic depiction of nanorod low-refractive-index thin film growth by oblique-angle deposition.

^{a)}Electronic mail: efschubert@rpi.edu

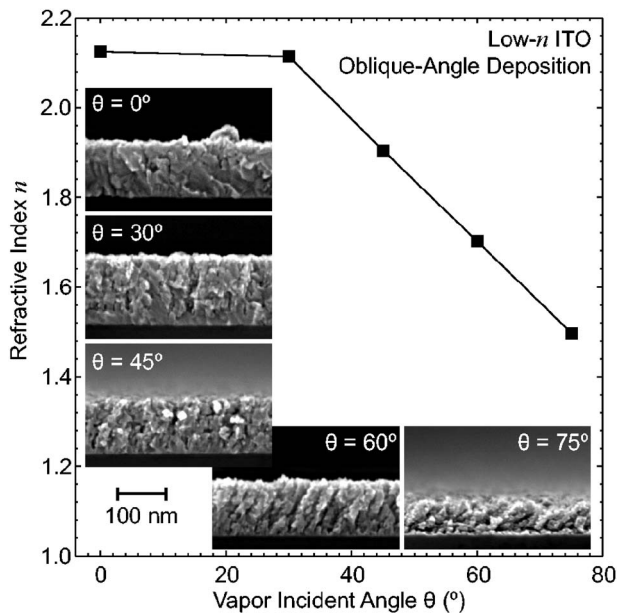


FIG. 2. Refractive index at $\lambda=460$ nm of ITO thin films as a function of the vapor incident angle. Inset images show cross section scanning-electron micrographs of the films.

film are small compared to a wavelength, it may be described by a homogenous refractive index whose value lies between that of air and the bulk material. As the vapor incident angle approaches 90° the self-shadowed areas increase and a more porous film is produced, which results in a lower refractive index. The complex refractive index and layer thickness are measured by ellipsometry. The layer-thickness result is confirmed by SEM.

The real part of refractive index is fitted with a three-term Cauchy model given by

$$n(\lambda) = A_n + \frac{B_n}{\lambda^2} + \frac{C_n}{\lambda^4}. \quad (1)$$

Figure 2 shows the refractive index at 460 nm of the ITO films for several incident angles. As the deposition angle increases, the refractive index becomes smaller and reaches a value of approximately 1.5 at 75° . The extinction coefficient is fitted with an expression of the form

$$k(\lambda) = A_k \exp \left[-B_k \left(\frac{1}{\lambda_0} - \frac{1}{\lambda} \right) \right]. \quad (2)$$

The extinction coefficient is close to the ITO bulk value for normal incidence and decreases as the incident angle increases, consistent with the increasing porosity of the films, which indicates that scattering loss within the nanorod layer is small. The Fig. 2 inset shows cross section SEM images of the ITO films which clearly demonstrate the decrease in density and formation of ITO nanorods. The nanorod feature size is smaller than 50 nm, i.e., much smaller than the wavelength of light. The small nanorod dimension suggests that Mie and Rayleigh scatterings can be neglected and the layer can be treated as a single homogeneous film with uniform refractive index.

DBR structures with one, two, and three periods are deposited on silicon substrates. The low-index layers consist of ITO deposited at an angle of 75° with a refractive index of $1.497 + i0.0056$ at a wavelength of 460 nm. The highest refractive index is achieved for bulk ITO deposited at normal

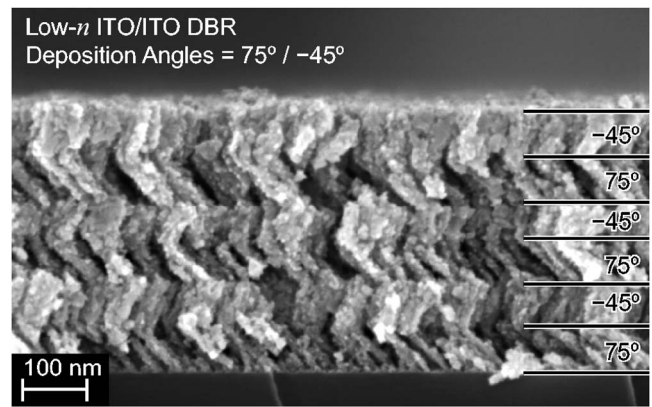


FIG. 3. Cross section scanning-electron micrograph of three-period DBR structure on a silicon substrate.

incidence. However, depositing a new layer at a near-normal vapor incident angle on top of a highly porous nanorod film could result in the filling in of a certain amount of space between the nanorods. To avoid this potential issue, the high-index layers are deposited at an incident angle of -45° which yields a refractive index of $1.904 + i0.0196$ at 460 nm. Figure 3 shows a cross section SEM image of the three-period ITO DBR. The nanorods layers have feature sizes much smaller than a wavelength and exhibit well defined interfaces. As a result, the DBR is expected to have reflection characteristics that show good agreement with theory. The expected conductive nature of the ITO DBR is verified by current-voltage measurements.

Figure 4 shows an optical micrograph of the one-, two-, and three-period DBRs. The three samples each have a featureless and highly specular surface. The one-period DBR has a silver color which indicates similar reflection throughout the visible wavelength range, while the two- and three-period DBRs have a pronounced bluish color. This is due to the enhanced reflection near the DBR center wavelength of 460 nm.

The wavelength-dependent reflectivity of the DBR samples is measured using a photospectrometer from 300 to 550 nm and is shown in Fig. 5 and compared with the theoretical reflection spectra for DBRs with the optimal $\lambda/(4n)$ layer thickness. For all samples the peak reflectivity is near the target wavelength of 460 nm. The reflectivity at



FIG. 4. (Color online) Optical micrograph of one-, two-, and three-period DBR samples. The two- and three-period DBRs have a bluish color, which indicates higher reflectivity in that wavelength range.

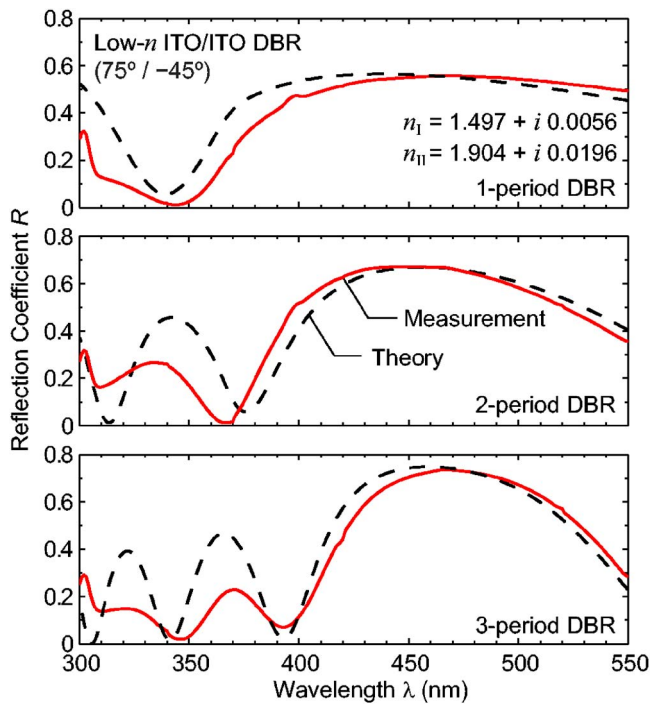


FIG. 5. (Color online) Measured and theoretical power reflection coefficient as a function of wavelength for the one-, two-, and three-period DBR structures. The target center wavelength is 460 nm.

460 nm is measured to be 55.5%, 67.0%, and 72.7% for the one-, two-, and three-period structures, which agrees well with the calculated reflectivity of 55.8%, 67.0%, and 74.8%. Secondary maxima of the reflection coefficient are somewhat lower than the predicted result. These maxima are the result of higher-order interference and are more sensitive to small deviations from the ideal layer thickness. However, locations of these maxima and the general shape of the reflection coefficient curve are in agreement with the theoretical result. The agreement between measurements and theoretical predictions indicates excellent refractive index and layer-thickness control.

In conclusion, a class of optical components is introduced that consists of only a single material used in multiple layers each having a different refractive index. Oblique-angle deposition decouples the refractive index from other material properties and thus allows the refractive index to be continuously varied over a broad range, thereby enabling compo-

nents such as the ITO-based conductive DBR demonstrated here. The three-period DBR achieves a reflectivity of 72.7% at $\lambda=460$ nm which is in very good agreement with theory. The combination of conductivity and index contrast of the low- n ITO DBR, facilitated by oblique-angle deposition, cannot be easily duplicated by conventional two-material approaches.

The authors gratefully acknowledge support from Sandia National Laboratories, Crystal IS Corporation, Samsung Advanced Institute of Technology (SAIT), Army Research Office (ARO), New York State Office of Science, Technology and Academic Research (NYSTAR), National Science Foundation (NSF), and the Department of Energy (DOE).

- ¹J.-Q. Xi, J. K. Kim, and E. F. Schubert, *Nano Lett.* **5**, 1385 (2005).
- ²W. H. Southwell, *Opt. Lett.* **8**, 584 (1983).
- ³J. A. Dobrowolski, D. Poitras, P. Ma, H. Vakil, and M. Acree, *Appl. Opt.* **41**, 3075 (2002).
- ⁴D. Poitras and J. A. Dobrowolski, *Appl. Opt.* **43**, 1286 (2004).
- ⁵J.-Q. Xi, M. Ojha, J. L. Plawsky, W. N. Gill, J. K. Kim, and E. F. Schubert, *Appl. Phys. Lett.* **87**, 031111 (2005).
- ⁶J.-Q. Xi, M. Ojha, W. Cho, J. L. Plawsky, W. N. Gill, T. Gessmann, and E. F. Schubert, *Opt. Lett.* **30**, 1518 (2005).
- ⁷R. Sharma, E. D. Haberer, C. Meier, E. L. Hu, and S. Nakamura, *Appl. Phys. Lett.* **87**, 051107 (2005).
- ⁸S.-T. Ho, S. L. McCall, R. E. Slusher, L. N. Pfeiffer, K. W. West, A. F. J. Levi, G. E. Blonder, and J. L. Jewell, *Appl. Phys. Lett.* **57**, 1387 (1990).
- ⁹Q. Xu, V. R. Almeida, R. R. Panepucci, and M. Lipson, *Opt. Lett.* **29**, 1626 (2004).
- ¹⁰M. Schmidt, G. Boettger, M. Eich, W. Morgenroth, U. Huebner, R. Boucher, H. G. Meyer, D. Konjhodzic, H. Bretinger, and F. Marlow, *Appl. Phys. Lett.* **85**, 16 (2004).
- ¹¹J. K. Kim, T. Gessmann, E. F. Schubert, J.-Q. Xi, H. Luo, J. Cho, C. Sone, and Y. Park, *Appl. Phys. Lett.* **88**, 013501 (2006).
- ¹²A. Jain, S. Rogojevic, S. Ponoht, N. Agarwal, I. Matthew, W. N. Gill, P. Persans, M. Tomozawa, J. L. Plawsky, and E. Simonyi, *Thin Solid Films* **398-399**, 513 (2001).
- ¹³K. Robbie, A. J. P. Hnatiw, M. J. Brett, R. I. MacDonald, and J. N. McMullin, *Electron. Lett.* **33**, 1213 (1997).
- ¹⁴K. Kaminska and K. Robbie, *Appl. Opt.* **43**, 1570 (2004).
- ¹⁵A. C. van Popta, M. M. Hawkeye, J. C. Sit, and M. J. Brett, *Opt. Lett.* **29**, 2545 (2004).
- ¹⁶T. Kato, H. Susawa, M. Hirotsu, T. Saka, Y. Ohashi, E. Shichi, and S. Shibata, *J. Cryst. Growth* **107**, 832 (1991).
- ¹⁷S. Chiou, C. Lee, C. Huang, and C. Chen, *J. Appl. Phys.* **87**, 2052 (2000).
- ¹⁸J. Xu, H. Fang, and Z. Lin, *J. Phys. D* **34**, 445 (2001).
- ¹⁹D. Huffaker, L. Graham, H. Deng, and D. Deppe, *IEEE Photonics Technol. Lett.* **8**, 974 (1996).
- ²⁰D. Winston and R. Hayes, *IEEE J. Quantum Electron.* **34**, 707 (1998).